

# Cosmological implications and structure formation from a time varying vacuum

Spyros Basilakos

*Academy of Athens, Research Center for Astronomy & Applied Mathematics, Soranou Efessiou 4, 11-527, Athens, Greece*

31 October 2018

## ABSTRACT

We study the dynamics of the FLRW flat cosmological models in which the vacuum energy varies with time,  $\Lambda(t)$ . In this model we find that the main cosmological functions such as the scale factor of the universe and the Hubble flow are defined in terms of exponential functions. Applying a joint likelihood analysis of the recent supernovae type Ia data, the Cosmic Microwave Background shift parameter and the Baryonic Acoustic Oscillations traced by the Sloan Digital Sky Survey (SDSS) galaxies, we place tight constraints on the main cosmological parameters of the  $\Lambda(t)$  scenario. Also, we compare the  $\Lambda(t)$  model with the traditional  $\Lambda$  cosmology and we find that the former model provides a Hubble expansion which compares well with that of the  $\Lambda$  cosmology. However, the  $\Lambda(t)$  scenario predicts stronger small scale dynamics, which implies a faster growth rate of perturbations with respect to the usual  $\Lambda$ -cosmology, despite the fact that they share the same equation of state parameter. In this framework, we find that galaxy clusters in the  $\Lambda(t)$  model appear to form earlier than in the  $\Lambda$  model.

**Keywords:** cosmology: theory - large-scale structure of universe

## 1 INTRODUCTION

The detailed analysis of the available high quality cosmological observations (Riess et al. 1998; Perlmutter et al. 1999; Efstathiou et al. 2002; Basilakos & Plionis 2005; Tegmark et al. 2006; Davis et al. 2007, Kowalski et al. 2008; Komatsu et al. 2009) have converged during the last decade towards a cosmic expansion history that involves a spatial flat geometry and a recent accelerating expansion of the universe. This expansion has been attributed to an energy component (dark energy) with negative pressure which dominates the universe at late times and causes the observed accelerating expansion. The simplest type of dark energy corresponds to the cosmological constant (see for review Peebles & Ratra 2003). The nature of the dark energy is still a mystery and indeed it is one of the most fundamental current problems in physics and cosmology.

In the literature, there are many theoretical speculations regarding the physics of the above exotic dark energy. The simplest approach is to consider a real scalar field  $\phi$  which rolls down the potential energy  $V(\phi)$  and therefore it could mimic the dark energy (Ratra & Peebles 1988; Weinberg 1989; Turner & White 1997; Caldwell, Dave & Steinhardt 1998; Padmanabhan 2003). Alternatively, Ozer & Taha (1987) proposed a different scenario in which a time varying  $\Lambda$  parameter could be a possible candidate for the dark energy (see also Bertolami 1986; Freese et al. 1987; Peebles &

Ratra 1988; Carvalho, Lima & Waga 1992; Overduin & Cooperstock 1998; Bertolami & Martins 2000; Alcaniz & Maia 2003; Opher & Pellison 2004; Bauer 2005; Barrow & Clifton 2006; Montenegro & Carneiro 2007 and references therein). In this cosmological model the dark energy equation of state parameter  $w \equiv P_{DE}/\rho_{DE}$ , is strictly equal to -1, but the vacuum energy density (or  $\Lambda$ ) varies with time. It is interesting to mention here that the renormalization group (RG) in quantum field theory (Shapiro & Solá 2000; Babić et al. 2002) provides a time varying vacuum, in which the  $\Lambda$  component evolves as  $\sim H^2(t)$  [see Grande, Solá & Stefancic 2006], where  $H$  is the Hubble parameter. On the other hand, based on the holographic principle (Bousso 2002; Padmanabhan 2005) one can prove that  $\Lambda \sim H^4$ .

However, in the  $\Lambda(t)$  cosmological model there is a coupling between the time-dependent vacuum and matter (Carneiro et al. 2008). In particular, using the combination of the conservation of the total energy with the variation of the vacuum energy one can prove that the  $\Lambda(t)$  model provides either a process of a particle production or the mass of the dark matter particles increases. The latter general properties can be explained within the framework of the interacting dark energy models (Alcaniz & Lima 2005 and references therein). We would like to stress here that most of the recent papers in dark energy studies are based on the assumption that the dark energy evolves independently of the

dark matter. Of course, the unknown nature of both dark matter and dark energy implies that at the moment we can not exclude the possibility of interactions in the dark sector. The confirmation of such a possibility would be of paramount importance because interactions between dark matter and dark energy could provide possible solutions to the cosmological coincidence problem. In general, several papers have been published in this area (eg., Zimdahl, Pavón, Chimento 2001; Amendola et al. 2003; Cai & Wang 2005; Binder & Kremer 2006; Das, Corasaniti, & Khoury 2006; Olivares, Atrio-Barandela & Pavón 2008 and references therein) proposing that the dark energy and dark matter could be coupled.

The aim of the present work is to investigate the observational consequences of the overall dynamics by using the  $\Lambda(t)$  cosmological model. Due to the absence of a physically well-motivated functional form for the  $\Lambda(t)$  parameter, we consider a power series form in  $H$  up to a second order. Doing so, we include the effects of the de-Sitter spacetime. The plan of the paper is as follows. The basic theoretical elements of the problem are presented in section 2 by solving analytically [for a spatially flat Friedmann-Lemaître-Robertson-Walker (FLRW) geometry] the basic cosmological equations. In section 3 we place constraints on the main parameters of our model by performing a joint likelihood analysis utilizing the Union08 SNIa data (Kowalski et al. 2008), the shift parameter of the Cosmic Microwave Background (Komatsu et al. 2009) and the observed Baryonic Acoustic Oscillations (BAOs; Eisenstein et al. 2005; Padmanabhan, et al. 2007). Section 4 outlines the comparison between the time varying vacuum model with the traditional  $\Lambda$  cosmology. Also, in section 4 we solve analytically the time evolution equation of the mass density contrast for the  $\Lambda(t)$  model while in section 5 we present theoretical predictions regarding the formation of the galaxy clusters. In section 6 we draw our conclusions. Finally, in the appendix we have treated analytically, the basic cosmological equations considering that the time varying  $\Lambda(t)$  parameter can be expressed with the aid of a power series expansion in  $H$  up to a third order. Note, that throughout the paper we use  $H_0 = 70.5 \text{ Km/sec/Mpc}$  (Freedman et al. 2001; Komatsu et al. 2009).

## 2 COSMOLOGY WITH A TIME DEPENDENT VACUUM

In the framework, of a spatially flat Friedmann-Lemaître-Robertson-Walker (FLRW) geometry the basic equations which governs the global dynamics of the universe are

$$\rho_m + \rho_\Lambda = 3H^2 \quad (1)$$

and

$$\frac{d(\rho_m + \rho_\Lambda)}{dt} + 3H(\rho_m + P_m + \rho_\Lambda + P_\Lambda) = 0 \quad (2)$$

where  $\rho_m$  and  $\rho_\Lambda$  are the matter density and vacuum density respectively, while  $P_m = 0$  and  $P_\Lambda$  is the corresponding vacuum pressure. Note, that for simplicity we use geometrical units ( $8\pi G = c \equiv 1$ ) in which  $\rho_\Lambda = \Lambda$ .

In order to study the above system of differential equations we need to define explicitly the functional form of the  $\Lambda$  component. Within the framework of the  $\Lambda(t)$  model it is interesting to note that the equation of state takes the usual form of  $P_\Lambda = -\rho_\Lambda(t) = -\Lambda(t)$  [Ozer & Taha 1987; Peebles & Ratra 1988].

On the other hand, introducing in the global dynamics the above idea in a form of the time-dependent vacuum, it is possible to explain the physical properties of the dark energy. Considering now eq.(2), we have the following useful formula (see also Carneiro et al. 2008):

$$\dot{\rho}_m + 3H\rho_m = -\dot{\Lambda} \quad (3)$$

and indeed, using eq.(1), we obtain:

$$2\dot{H} + 3H^2 = \Lambda \quad (4)$$

or

$$\int_{+\infty}^H \frac{dy}{\Lambda - 3y^2} = \int_0^t \frac{du}{2} = \frac{t}{2} \quad (5)$$

where the over-dot denotes derivatives with respect to time. Of course, the traditional  $\Lambda$  cosmology can be described by the above integration (eq.5) using a constant vacuum term  $\Lambda = \text{const}$  (for more details see section 3.5).

Now, from eq.(3), it becomes evident that in this cosmological scenario there is a coupling between the time-dependent vacuum and matter. Actually, the idea for possible interactions in the dark sector is not really new in this kind of studies. It has been shown that the coupling between dark matter and dark energy could provide possible solutions to the cosmological coincidence problem (eg., Zimdahl, Pavón, Chimento 2001; Amendola et al. 2003; Cai & Wang 2005; Binder & Kremer 2006; Das, Corasaniti, & Khoury 2006; Olivares, Atrio-Barandela & Pavón 2008 and references therein). In this context, one of the most important issues and unknowns is the precise functional form of the equation of state parameter  $w(a)$  where ( $a$  is the scale factor). The usual procedure is to derive a  $w(a)$  approximate functional form, by using a Taylor expansion around the present epoch (eg. Chevalier & Polarski, 2001; Linder 2003), which then provides approximate solutions of the global density evolution. However, the current approach is somewhat different in the sense that we do not “design” the equation of state parameter such that to produce the desired (accelerated) cosmic evolution. Rather, we investigate whether a generalized vacuum component with  $w(t) = -1$  and  $P_\Lambda = -\rho_\Lambda(t)$  [Ozer & Taha 1987; Peebles & Ratra 1988] in the expanding Universe allows for a late accelerated phase of the Universe and under which circumstances such a solution provides a viable alternative to the dark energy.

Although, we do not have a fundamental theory to model the time-dependent  $\Lambda(t)$  function, we can parametrize the latter using a phenomenological approach. Indeed, in a series of recent papers, authors (see for example Ray, Mukhopadhyay & Meng 2007; Sil & Som 2008 and references therein) have investigated the global dynamical properties of the universe considering that the vacuum energy density decreases linearly either with the energy density or the square Hubble param-

ter. Also, Wang & Meng (2005), based on thermodynamics found that the vacuum energy density possibly decays as a power law. Alternatively, Carneiro et al. (2008) proposed a different pattern in which the vacuum term is proportional with the Hubble parameter,  $\Lambda(a) \propto H(a)$ . However, this model fails to fit the current CMB data (see also section 3.4). In this context, attempts to provide a theoretical explanation for the  $\Lambda(t)$  have been presented in the literature (see Grande et al. 2006 and references therein). These authors found that a time dependent vacuum could arise from the renormalization group (RG) in quantum field theory. The corresponding solution for a running  $\Lambda(t)$  is found to be  $\Lambda(t) \sim c_1 H^2(t)$  [where  $c_1$  is a constant] and it can mimic the quintessence or phantom behavior and transit smoothly between the two. It is worth noting that at late enough times the above solution asymptotically reaches the de-Sitter regime  $\Lambda \sim H^2$ , as far as the global dynamics is concerned.

In this paper, we parametrize the functional form of  $\Lambda(t)$  by applying a power series expansion in  $H$  up to the second order (see the appendix for a third order expansion which interestingly predict models with late acceleration but without initial singularities):

$$\Lambda(t) = n_1 H + n_2 H^2. \quad (6)$$

Obviously, eq.(6) can be seen as a combination of the of the above ansatz namely  $H(t)$  (Carneiro et al. 2008) and  $H^2(t)$  [quantum field theory; Grande et al. 2006] respectively. It is now routine to integrate eq.(5) and obtain the Hubble function predicted by the current  $\Lambda(t)$  model:

$$H(t) = \frac{n_1}{\beta} \frac{e^{n_1 t/2}}{e^{n_1 t/2} - 1}, \quad (7)$$

where the range of  $\beta (= 3 - n_2)$  values for which the above integration is valid is  $\beta \in (0, +\infty)$  (or  $n_2 < 3$ ). Of course, if we consider different patterns for the vacuum density then we can obtain different solutions for the Hubble parameter. Using now the definition of the Hubble parameter  $H \equiv \dot{a}/a$ , the scale factor of the universe  $a(t)$ , evolves with time as

$$a(t) = a_1 (e^{n_1 t/2} - 1)^{2/\beta}, \quad (8)$$

where  $a_1$  is the constant of integration. As expected, at late enough times the above solution reduces to the de-Sitter universe. Note, that for  $\beta \rightarrow 3$  and at early times the  $\Lambda(t)$  model tends to the Einstein de-Sitter case. Now from eqs.(7, 8) we can easily write the corresponding Hubble flow as a function of the scale factor

$$H(a) = \frac{n_1}{\beta} \left[ 1 + \left( \frac{a}{a_1} \right)^{-\beta/2} \right]. \quad (9)$$

Evaluating eq.(9) at the present time ( $a \equiv 1$ ) we obtain

$$n_1 = \frac{\beta H_0}{1 + a_1^{\beta/2}} \quad (10)$$

where  $H_0$  is the Hubble constant. From eqs.(9, 10), using the usual unit-less  $\Omega$ -parameterization, we have after some algebra that:

$$E(a) \equiv \frac{H(a)}{H_0} = (1 - \Omega_m + \Omega_m a^{-\beta/2}) \quad (11)$$

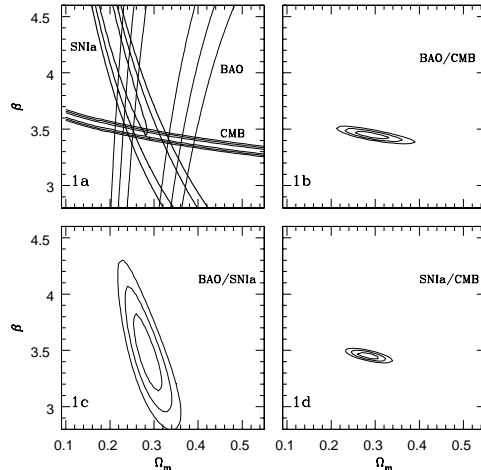


**Figure 1.** Likelihood contours in the  $(\Omega_m, \beta)$  plane. The contours are plotted where  $-2\ln(\mathcal{L}/\mathcal{L}_{\max})$  is equal to 2.32, 6.16 and 11.83, corresponding to  $1\sigma$ ,  $2\sigma$  and  $3\sigma$  confidence level. In Fig.1a we present the likelihood contours that correspond to the SNIa, CMB and BAOs observational data. Finally, Figs. 1b, 1c and 1d show the statistical results for different pairs.

while the corresponding matter density parameter is:  $\Omega_m(a) = \Omega_m a^{-\beta/2}/E(a)$ . The normalized scale factor of the universe becomes

$$a(t) = \left( \frac{\Omega_m}{1 - \Omega_m} \right)^{2/\beta} \left[ e^{\beta(1 - \Omega_m)H_0 t/2} - 1 \right]^{2/\beta} \quad (12)$$

or

$$t(a) = \frac{2}{\beta(1 - \Omega_m)} H_0^{-1} \ln \left[ \frac{a^{\beta/2} E(a)}{\Omega_m} \right] \quad (13)$$

where  $a_1^{\beta/2} = \Omega_m/(1 - \Omega_m)$ . It is interesting to point here that the current age of the universe [ $a = 1$ ,  $E(1) = 1$ ] is

$$t_0 = \frac{2}{\beta} H_0^{-1} \frac{\ln \Omega_m}{\Omega_m - 1}. \quad (14)$$

We now investigate the circumstances under which an inflection point exists and therefore have an acceleration phase of the scale factor. This crucial period in the cosmic history corresponds to  $\ddot{a}(t_I) = 0$ . Differentiating twice eq.(12), we then have:

$$a_I = \left[ \frac{(\beta - 2)\Omega_m}{2(1 - \Omega_m)} \right]^{2/\beta} \quad t_I = \frac{2}{\beta(1 - \Omega_m)} H_0^{-1} \ln \left( \frac{\beta}{2} \right) \quad (15)$$

which implies that the condition for which an inflection point is present in the evolution of the scale factor is  $\beta > 2$ .

### 3 COSMOLOGICAL CONSTRAINTS

#### 3.1 The likelihood from the CMB shift parameter

A very accurate and deep geometrical probe of dark energy is the angular scale of the sound horizon at the

last scattering surface as encoded in the location of the first peak of the Cosmic Microwave Background (CMB) temperature perturbation spectrum. This probe is described by the so called CMB shift parameter (cf. Bond, Efstathiou & Tegmark 1997; Trotta 2004; Nesseris & Perivolaropoulos 2007) which is a normalized quantity and it is defined as

$$R = \sqrt{\Omega_m} \int_{a_{l_s}}^1 \frac{da}{a^2 E(a)} = \sqrt{\Omega_m} \int_0^{z_{l_s}} \frac{dz}{E(z)} . \quad (16)$$

One of the merits of using the shift parameter in cosmological studies is that its dependence on the Hubble constant is negligible (for details see Melchiorri et al. 2003; Nesseris & Perivolaropoulos 2007 and references therein). The shift parameter measured from the WMAP 5-years data (Komatsu et al. 2009) is  $R = 1.71 \pm 0.019$  at  $z_{l_s} = 1090$  [or  $a_{l_s} = (1 + z_{l_s})^{-1} \simeq 9.17 \times 10^{-4}$ ] and  $E(z) \equiv H(z)/H_0$  is the normalized Hubble flow. Therefore, the corresponding  $\chi_{\text{cmb}}^2$  function is simply written

$$\chi_{\text{cmb}}^2(\mathbf{p}) = \frac{[R(\mathbf{p}) - 1.71]^2}{0.019^2} \quad (17)$$

where  $\mathbf{p}$  is a vector containing the cosmological parameters that we want to fit. Note, that we sample the unknown parameters as follows:  $\Omega_m \in [0.1, 1]$  and  $\beta \in [2, 5]$  in steps of 0.01. In Fig.1a we present the  $1\sigma$ ,  $2\sigma$  and  $3\sigma$  confidence levels in the  $(\Omega_m, \beta)$  plane. It is evident that the  $\beta$  parameter is tightly constrained ( $\beta \simeq 3.58$ ) while the matter density parameter is not and all the values in the interval  $0.1 \leq \Omega_m \leq 1$  are acceptable (see Table 1). However, following the WMAP 5-years results (Komatsu et al. 2009) of the full temperature perturbation spectrum  $\Delta T/T$ , we can use an additional constrain which is  $\Omega_m h^2 = 0.1326 \pm 0.0063$ . Thus, for  $h \simeq 0.71$  (Freedman et al. 2001; Komatsu et al. 2009) we find  $0.24 \leq \Omega_m \leq 0.29$  ( $2\sigma$  limits).

### 3.2 The likelihood from the SNIa

We now use the publicly available Union08 sample of 307 supernovae of Kowalski et al. (2008) in order to

constrain  $\Omega_m^*$ . In this case, the likelihood function can be written as:

$$\chi_{\text{SNIa}}^2(\mathbf{p}) = \sum_{i=1}^{307} \left[ \frac{\mu^{\text{th}}(a_i, \mathbf{p}) - \mu^{\text{obs}}(a_i)}{\sigma_i} \right]^2 . \quad (18)$$

where  $a_i = (1 + z_i)^{-1}$  is the observed scale factor of the universe,  $z_i$  is the observed redshift,  $\mu$  is the distance modulus  $\mu = m - M = 5 \log d_L + 25$  and  $d_L(a, \mathbf{p})$  is the luminosity distance

$$d_L(a, \mathbf{p}) = \frac{c}{H_0 a} \int_a^1 \frac{dx}{x^2 E(x)} \quad (19)$$

where  $c$  is the speed of light ( $\equiv 1$  here). Figure 1a also shows the  $1\sigma$ ,  $2\sigma$  and  $3\sigma$  confidence levels in the  $(\Omega_m, \beta)$  plane. Although, the  $\beta$  parameter is not constrained by this analysis the matter density parameter has an upper limit of  $\Omega_m \leq 0.29$  within the  $1\sigma$  uncertainty (see Table 1).

### 3.3 The likelihood from BAOs

In this section, we utilize the so called Baryonic Acoustic Oscillations. BAOs are produced by pressure (acoustic) waves in the photon-baryon plasma in the early universe, generated by dark matter overdensities. Evidence of this excess has been found in the clustering properties of the luminous SDSS red-galaxies (Eisenstein et al. 2005; Padmanabhan, et al. 2007) and it can provide a "standard ruler" with which we can put constraints on the cosmological models. In particular, we use the following estimator:

$$A(\mathbf{p}) = \frac{\sqrt{\Omega_m}}{[z_s^2 E(a_s)]^{1/3}} \left[ \int_{a_s}^1 \frac{da}{a^2 E(a)} \right]^{2/3} \quad (20)$$

measured from the SDSS data to be  $A = 0.469 \pm 0.017$ , where  $z_s = 0.35$  [or  $a_s = (1 + z_s)^{-1} \simeq 0.75$ ]. In this case, the  $\chi_{\text{BAO}}^2$  function is given

$$\chi_{\text{BAO}}^2(\mathbf{p}) = \frac{[A(\mathbf{p}) - 0.469]^2}{0.017^2} . \quad (21)$$

\* <http://supernova.lbl.gov/Union>. This catalog includes the following components in the error budget of the distance moduli: (a)  $\sigma_{\text{tot}}$ , (see Kowalski et al. 2008) obtained due to lensing, Milky way dust extinction and host galaxy peculiar velocities (b) the systematic error  $\sigma_{\text{sys}}$  and (c) the uncertainty which is related with the light-curve fitting. For the latter uncertainty, Kowalski et al. take into account the stretch  $s$  and color  $c$  corrections via  $\mu_B = m_B - M + \alpha(s-1) - bc$  for a specific cosmological model  $(\Omega_m, w) = (0.29, -0.97)$ . We would like to caution the reader that we do not minimize  $\chi^2$  over the parameters  $\alpha$  and  $b$ , which implies that in the case of the  $\Lambda(t)$  model we may not be treating the third component of the error budget properly. However, we would like to stress that according to Kowalski et al. (2008) the corresponding constants  $\alpha$  and  $b$  are rather insensitive to the assumed cosmological parameters (see their section 5.1). Thus, had we included the proper light-curve uncertainty in our fit we would have obtained a larger solution space (see figure 1a).

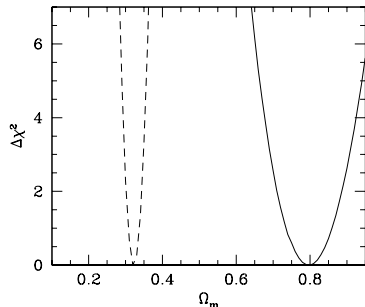


**Figure 2.** The variance  $\Delta\chi^2 = \chi^2 - \chi_{min}^2$  around the best fit  $\Omega_m$  value when we marginalize over  $\beta = 3$  [ $\Lambda(t) \propto H(t)$ ]. The solid and the dashed line corresponds to the CMB and SNIa/BAO likelihoods respectively.

It is evident (see figure 1a), that the matter density parameter is constrained ( $\Omega_m \simeq 0.28$ ) by this analysis, while the  $\beta$  parameter is not (see also Table 1).

### 3.4 The joint likelihoods

We can combine the above probes by using a joint likelihood analysis:

$$\mathcal{L}_{tot}(\mathbf{p}) = \mathcal{L}_{BAO} \times \mathcal{L}_{cmb} \times \mathcal{L}_{SNIa}$$

or

$$\chi_{tot}^2(\mathbf{p}) = \chi_{BAO}^2 + \chi_{cmb}^2 + \chi_{SNIa}^2$$

in order to put even further constraints on the parameter space used. Note, that we define the likelihood estimator<sup>†</sup> as:  $\mathcal{L}_j \propto \exp[-\chi_j^2/2]$ . The resulting best fit parameters, are presented in the second two rows of Table 1. The overall likelihood function peaks at  $\Omega_m = 0.29^{+0.01}_{-0.02}$ ,  $\beta = 3.44 \pm 0.02$  and the corresponding  $\chi_{tot}^2(\Omega_m, \beta)$  is 310.2 (dof = 307). In this cosmological scenario the current age of the universe is found to be  $t_0 \simeq 14.1$ Gyr and the inflection point is located at  $(a_I, t_I) \simeq (0.49, 0.44t_0)$ . In Figs. 1b, 1c and 1d we present, for various observational pairs, the corresponding likelihood contours (see also Table 1).

Finally, it is worth noting that Carneiro et al. (2008) considered a different ansatz in order to parametrize the time dependence of the vacuum energy. Their assumption is based on the fact that  $\Lambda(t)$  is proportional to the Hubble parameter (in our formulation  $n_2 = 0$ ). They found that this model fits the observational data (BAO+SNIa+CMB) at  $2\sigma$  level for  $\Omega_m \simeq 0.43$ . In our case, if we marginalize over  $\beta = 3$  (or  $n_2 = 0$ ), then the joint likelihood analysis provides a best fit value of  $\Omega_m \simeq 0.35$ , but the fit is rather poor  $\chi_{tot}^2(\Omega_m) \simeq 383$  (dof = 308). We investigate a bit further this result and we reveal that the poor joint fit is due to the fact that the best fit value provided by the likelihood analysis of CMB shift parameter is found

to be more than  $3\sigma$  away,  $\Omega_m \simeq 0.80$  (see solid line in figure 2), from the SNIa/BAO solution  $\Omega_m \simeq 0.32$  (see dashed line in figure 2). This implies that the functional form  $E(a) = 1 - \Omega_m + \Omega_m a^{-3/2}$  fails to fit the CMB data. We thus argue that the  $\Lambda(t) \propto H(t)$  relation produces a discrepancy between the SNIa/BAO and CMB shift parameter which may lead to misleading cosmological results. We further confirm the latter result, by using a Bayesian statistics (see for example Davis et al. 2007), in which the corresponding estimator is defined as:  $BIC = \chi^2 + k \ln N$  (where  $k$  is the number of parameters and  $N$  is the number of data points used in the fit). The next step is to estimate the relative deviation between the two models  $\Delta BIC = BIC^{n_1 H} - BIC^{n_1 H + n_2 H^2}$ . In general a difference in  $BIC$  of  $\Delta BIC > 6$ , is considered strong evidence against that model which occurs the larger  $BIC$ . In our case, we find  $\Delta BIC \simeq 69$  which implies a strong evidence against the  $\Lambda(t) \propto H(t)$  model.

### 3.5 The standard $\Lambda$ -Cosmology

In this section, we wish to remind the reader of some basic elements of the concordance  $\Lambda$ -cosmology in order to appreciate the differences with the  $\Lambda(t)$  cosmology. In the case of  $\Lambda = const$ , it is straightforward to integrate eq.(5). Therefore, the Hubble function predicted by the  $\Lambda$  model is

$$H(t) = \sqrt{\frac{\Lambda}{3}} \coth \left( \frac{3}{2} \sqrt{\frac{\Lambda}{3}} t \right) \quad (22)$$

where  $\Lambda = 3H_0^2(1 - \Omega_m)$ . Then the normalized Hubble function is written as

$$E_\Lambda(a) = \frac{H(a)}{H_0} = [1 - \Omega_m + \Omega_m a^{-3}]^{1/2} \quad (23)$$

while  $\Omega_m(a) = \Omega_m a^{-3}/E_\Lambda^2(a)$ . To this end, the scale factor of the universe is given by

$$a_\Lambda(t) = \left( \frac{\Omega_m}{1 - \Omega_m} \right)^{1/3} \sinh^{2/3} \left( \frac{3H_0\sqrt{1 - \Omega_m}t}{2} \right) \quad (24)$$

or

$$t_\Lambda(a) = \frac{2}{3\sqrt{1 - \Omega_m}} H_0^{-1} \ln \left[ \frac{\sqrt{1 - \Omega_m} + E_\Lambda(a)}{a^{-3/2}\sqrt{\Omega_m}} \right]. \quad (25)$$

Comparing the  $\Lambda$  model with the observational data we find that the best fit value is  $\Omega_m = 0.28 \pm 0.02$  with  $\chi_{tot}^2(\Omega_m) \simeq 308.5$  (dof = 308) in a good agreement with the 5 years WMAP data (Komatsu et al. 2009). Note, that Davis et al. (2007) using the Essence-SNIa+BAO+CMB and a Bayesian statistics found  $\Omega_m = 0.27 \pm 0.04$ , while Kowalski et al. (2008) utilizing the Union08-SNIa+BAO+CMB obtained  $\Omega_m = 0.274^{+0.016+0.013}_{-0.016-0.012}$  (for  $w \sim -1$ ). Obviously, our results coincide within  $1\sigma$  errors.

The current age of the universe is given by

$$t_{0\Lambda} = \frac{2}{3\sqrt{1 - \Omega_m}} H_0^{-1} \ln \left( \frac{\sqrt{1 - \Omega_m} + 1}{\sqrt{\Omega_m}} \right) \quad (26)$$

<sup>†</sup> Likelihoods are normalized to their maximum values. Note that the errors of the fitted parameters represent  $1\sigma$  uncertainties.

**Table 1.** Results of the likelihood function analysis. The 1<sup>st</sup> column indicates the data used (the last two rows corresponds to the inflection points). Errors of the fitted parameters represent 1 $\sigma$  uncertainties. Finally, the current age of the universe  $t_0$  has units of Gyr (for  $H_0 = 70.5\text{Km/sec/Mpc}$ ).

Sample	$\Omega_m$	$\beta$	$t_0$	$a_I$	$t_I/t_0$
CMB	uncons. ( $\Omega_m = 0.13$ )	$3.58^{+0.04}_{-0.32}$	18.2	0.30	0.29
SNIa	$0.20^{+0.12}_{-0.01}$	uncons. ( $\beta = 4.6$ )	12.4	0.59	0.50
BAO	$0.28^{+0.11}_{-0.04}$	uncons. ( $\beta = 3.50$ )	16.0	0.36	0.33
SNIa-BAO	$0.28^{+0.03}_{-0.02}$	$3.50^{+0.30}_{-0.36}$	14.0	0.49	0.44
CMB-BAO	$0.29^{+0.04}_{-0.03}$	$3.44^{+0.02}_{-0.02}$	14.1	0.49	0.44
SNIa-CMB	$0.29^{+0.01}_{-0.03}$	$3.44^{+0.02}_{-0.02}$	14.1	0.49	0.44
ALL	$0.29^{+0.01}_{-0.02}$	$3.44^{+0.02}_{-0.02}$	14.1	0.49	0.44

while the inflection point takes place at

$$t_{I\Lambda} = \frac{2}{3\sqrt{1-\Omega_m}} H_0^{-1} \ln \left( \frac{\sqrt{5}+1}{2} \right)$$

$$a_{I\Lambda} = \left[ \frac{\Omega_m}{2(1-\Omega_m)} \right]^{1/3}. \quad (27)$$

Therefore, we estimate  $t_{0\Lambda} \simeq 13.9\text{Gyr}$ ,  $t_{I\Lambda} \simeq 0.52t_{0\Lambda}$  and  $a_{I\Lambda} \simeq 0.58$ . Finally, using the previously described Bayesian statistics we find that  $\Delta BIC = BIC^{n_1 H + n_2 H^2} - BIC^\Lambda \simeq 5$ . This comparison implies a preference for the usual  $\Lambda$  cosmology.

#### 4 COMPARISON BETWEEN DIFFERENT TYPES OF VACUUM

In this section, we investigate in more detail the correspondence of the  $\Lambda(t)$  model with the traditional  $\Lambda$ -cosmology (see previous sections) in order to show the extent to which they compare.

##### 4.1 Compare the cosmic evolution

Knowing now the parameter space  $(\Omega_m, \beta)$  we present the evolution of the  $\Lambda(t)$  scale factor seen in the upper panel of figure 3 as the solid line. It can be seen that it closely resembles the corresponding scale factor of the  $\Lambda$  cosmology (dashed line). We have checked the cosmic phases of the  $\Lambda(t)$  scenario against the concordance cosmology by utilizing the deceleration parameter,  $q(a) = -(1 - a \ln H / da)$ . The evolution of the deceleration parameter is presented in the bottom panel of figure 3, while in the insert figure we plot the relative deviation of the deceleration parameter,  $\Delta(q - q_\Lambda)$ , between the two vacuum models. We find the following phases: (a) at early enough times  $a < 0.21$  the deceleration parameters are both positive with  $q > q_\Lambda$ , which means that the cosmic expansion in the  $\Lambda(t)$  model is more rapid decelerated than in the  $\Lambda$  case, (b) between  $0.21 < a < 0.49$  the deceleration parameters remain positive but  $q < q_\Lambda$ , (c) then for  $0.49 < a < 0.58$  the traditional  $\Lambda$  model remains in the decelerated regime  $q_\Lambda > 0$  but the  $\Lambda(t)$  is starting to accelerate  $q < 0$  and (d) for  $0.58 < a < 0.80$  the deceleration parameters are both negative and as long as  $q < q_\Lambda$  the  $\Lambda(t)$  model predicts a much more acceleration than in the  $\Lambda$

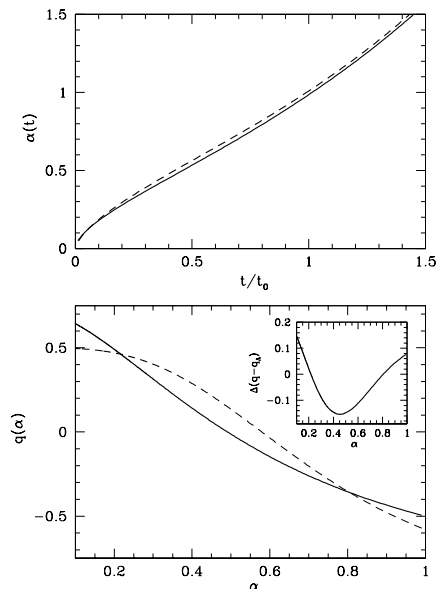


**Figure 3.** *Upper Panel:* Comparison of the scale factor provided by the  $\Lambda(t)$  model (solid line) with the traditional  $\Lambda$  cosmology (dashed line). *Bottom Panel:* The evolution of the deceleration parameter. In the insert panel we present the relative deviation  $\Delta(q - q_\Lambda)$  of the deceleration parameters.

model (the opposite situation seems to hold prior to the present epoch  $0.80 < a \leq 1$ ). In a special case where  $\Delta(q - q_\Lambda) = 0$  [ $q = q_\Lambda$ , either at  $a \simeq 0.21$  or  $a \simeq 0.80$ ] the two vacuum models predict exactly the same expansion of the universe. From figure 3 it becomes clear that the  $\Lambda(t)$  model reaches a maximum deviation from the  $\Lambda$  cosmology prior to  $a \sim 0.1$  ( $z \sim 9$ ) and  $a \sim 0.45$  ( $z \sim 1.2$ ). Therefore, in order to investigate whether the expansion of the observed universe follows one of the above possibilities, we need a robust extragalactic distance indicator at redshifts  $z > 1.2$ . Finally, the deceleration parameters at the present time are  $q_0 \simeq -0.50$  and  $q_{0\Lambda} \simeq -0.57$ .

##### 4.2 Compare the linear growth factor

In the framework of a time varying vacuum, the corresponding time evolution equation for the mass density contrast, in a pressureless fluid is given by (Arcuri & Waga 1994; see also Borges et al. 2008):

**Table 2.** Cosmological data of the growth rate of clustering (see Nesseris & Perivolaropoulos 2008). The correspondence of the columns is as follows: redshift, observed growth rate and references.

$z$	$f_{obs}$	Refs.
0.15	$0.51 \pm 0.11$	Verde et al. 2002; Hawkins et al. 2003
0.35	$0.70 \pm 0.18$	Tegmark et al. 2006
0.55	$0.75 \pm 0.18$	Ross et al. 2006
1.40	$0.90 \pm 0.24$	da Angela 2006
3.00	$1.46 \pm 0.29$	McDonald 2005

$$\ddot{D} + (2H + Q)\dot{D} - \left[ \frac{\rho_m}{2} - 2HQ - \dot{Q} \right] D = 0 \quad (28)$$

where  $\rho_m = 3H^2 - \Lambda$  (see eq.1) and  $Q(t) = -\dot{\Lambda}/\rho_m$ . It becomes clear, that the interacting vacuum energy affects the growth factor via the function  $Q(t)$ . Obviously, in the case of a constant  $\Lambda$  [ $Q(t) = 0$ ], the above equation reduces to the usual time evolution equation for the mass density contrast (see Peebles 1993). In this context, the growing solution as a function of redshift is given by:

$$D_\Lambda(z) = \frac{5\Omega_m E_\Lambda(z)}{2} \int_z^\infty \frac{(1+x)}{E_\Lambda^3(x)} dx \quad (29)$$

We now proceed in an attempt to analytically solve eq.(28). To do so, we change variables from  $t$  to a new one following the transformation

$$y = \exp(n_1 t/2) \quad 0 < y < 1 \quad (30)$$

Doing so, eq.(28) can be written:

$$\beta^2 y (y-1)^2 D'' + 2\beta(y-1)(5y-\beta) D' - 2(6-\beta)(\beta-2y) D = 0 \quad (31)$$

where prime denotes derivatives with respect to  $y$ . We find that eq.(31) has a decaying solution for  $\beta < 8$  of the form  $D_1(y) = (y-1)^{(\beta-6)/\beta}$ . The second independent solution (growing mode) of eq.(31) can be found easily from the following expression:

$$D(y) = D_1(y) \int_y^1 \frac{(u-1)^{2/\beta} du}{u^2} \quad (32)$$

Inserting eq.(10) and eq.(13) into eq.(30), the  $y$  variable is related with the scale factor as:

$$y = \frac{a^{\beta/2}(1-\Omega_m) + \Omega_m}{\Omega_m} \quad (33)$$

In the redshift regime [ $a = (1+z)^{-1}$ ] the combination of the above two equations lead to the following growing mode:

$$D(z) = C(\Omega_m)(1+z)^{(6-\beta)/2} \int_z^\infty \frac{(x+1)^{(\beta-4)/2} dx}{E^2(x)} \quad (34)$$

where

$$C(\Omega_m) = \frac{\beta}{2} \Omega_m^2 \left( \frac{1-\Omega_m}{\Omega_m} \right)^{(2\beta-4)/\beta} \quad (35)$$

In the upper panel of figure 4 we present the growth factor evolution, derived by integrating eq.(29) and eq.(34), for the two vacuum models. Note that the growth factors are normalized to unity at the present time. Despite the fact that the global cosmological behavior of the  $\Lambda(t)$  vacuum model is in a good agreement

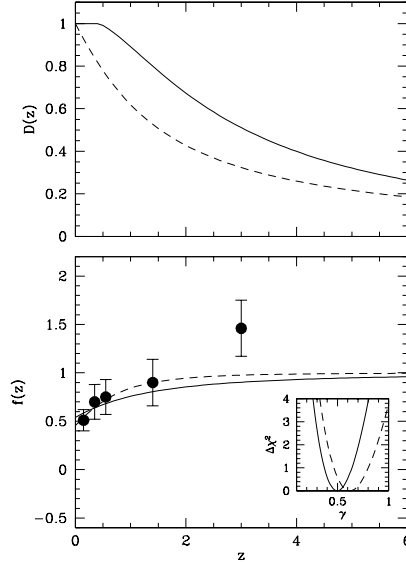


**Figure 4.** Upper Panel: The evolution of the growth factor for different vacuum models. The lines correspond to  $\Lambda(t)$  (solid) and  $\Lambda$  (dashed). Bottom Panel: Comparison of the observed and theoretical evolution of the growth rate of clustering  $f(z)$ . Note, that data can be found in Nesseris & Perivolaropoulos (2008). The best fit for the  $\Lambda(t)$  model shows a  $\sim 10\%$  difference from the traditional  $\Lambda$  model, especially at large redshifts.

with the usual  $\Lambda$  cosmology (as it seen in figure 3), the two vacuum cosmological models trace differently the evolution of the matter fluctuation field. In particular, close to the present epoch ( $z < 0.3$ ) the  $\Lambda(t)$  growth factor reaches a plateau, which means that the matter fluctuations are effectively frozen. It is obvious that the growth factor in the  $\Lambda(t)$  model is much greater than that of the concordance  $\Lambda$  cosmology. Indeed, assuming that clusters of galaxies have formed prior to the epoch of  $z \simeq 1.4$  ( $a \sim 0.42$ ), in which the most distant cluster has been found (Mullis et al. 2005; Stanford et al. 2006), the deviation  $(1 - D/D_\Lambda)\%$ , of the growth factor  $D(a)$  for the  $\Lambda(t)$  scenario with respect to the  $\Lambda$  solution  $D_\Lambda(a)$  is  $-51\%$  while prior to the inflection point ( $a_I \sim 0.5$ ) we find  $-43\%$ . We conclude that the behavior of the growth factor is sensitive to the different types of vacuum with  $D(z) > D_\Lambda(z)$  and it is expected that this difference will affect also the predictions related with the formation of the cosmic structures (see section 5).

### 4.3 Compare the growth rate of clustering

We further compare the two vacuum cosmological scenarios by utilizing the well known indicator of clustering, namely the growth rate  $f(a) \equiv d \ln D / d \ln a$  (Peebles 1993). The corresponding parametrization of the growth rate of clustering can be achieved by introducing a growth index  $\gamma$  (see Wang & Steinhardt 1998) defined by

$$f(a) = \Omega_m^\gamma(a) \quad (36)$$

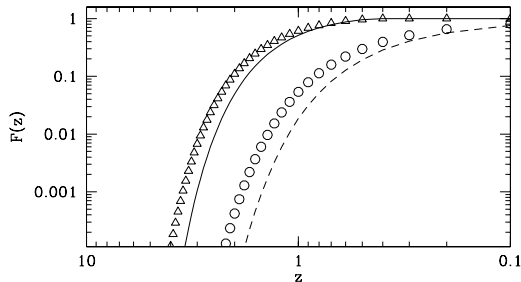


**Figure 5.** Theoretical predictions of the fractional rate of cluster formation as a function of redshift. Note, that the solid and dashed line corresponds to  $\Lambda(t)$  and usual  $\Lambda$  cosmological model respectively ( $\sigma_8 = 0.80$ ). Finally, for  $\sigma_8 = 0.95$  we get: (i) the open triangles for  $\Lambda(t)$  and (ii) open circles for  $\Lambda$ .

In order to quantify the growth index we perform a standard  $\chi^2$  minimization procedure (described previously) between the measured growth rate of the 2dF and SDSS catalogs (see Table 2; Nesseris & Perivolaropoulos 2008) with those expected in our spatially flat cosmological models

$$\chi^2(\gamma) = \sum_{i=1}^5 \left[ \frac{f_{obs}(z_i) - f_{model}(z_i, \gamma)}{\sigma_i} \right]^2, \quad (37)$$

where  $\sigma_i$  is the observed growth rate uncertainty. In the bottom panel of figure 4, we present the measured  $f_{obs}(z)$  (filled symbols) with the estimated growth rate function  $f(z) = \Omega_m^\gamma(z)$  for the considered cosmological models. Notice, that for the  $\Lambda(t)$  model (solid line) we use  $(\Omega_m, \beta) = (0.29, 3.44)$  and for the  $\Lambda$  case (dashed line) we impose  $\Omega_m = 0.28$ . Also, in the insert panel of figure 4 we plot the variation of  $\Delta\chi^2 = \chi^2(\gamma) - \chi_{min}^2(\gamma)$  around the best  $\gamma$  fit. We find that the growth index is  $\gamma = 0.50^{+0.14}_{-0.12}$  ( $\chi^2/\text{dof} = 1.14$ ) for the  $\Lambda(t)$ , which is somewhat less (but still within  $1\sigma$  errors) than the  $\Lambda$  growth index,  $\gamma_\Lambda = 0.62^{+0.18}_{-0.15}$  ( $\chi^2/\text{dof} = 0.75$ ).

## 5 THE FORMATION OF GALAXY CLUSTERS

In this section we attempt to briefly investigate the cluster formation processes by generalizing the basic equations which govern the behavior of the matter perturbations within the framework of a  $\Lambda(t)$  flat cosmology. Also we compare our predictions with those found for the traditional  $\Lambda$  cosmology. This can help us to understand better the theoretical expectations of the  $\Lambda(t)$  cosmological scenario as well as the variants from the  $\Lambda$  model.

The concept of estimating the fractional rate of cluster formation has been brought up by different authors (cf. Peebles 1984; Weinberg 1987; Martel & Wasserman 1990; Richstone, Loeb & Turner 1992). The above authors introduced a methodology which computes the rate at which mass joins virialized structures, which grow from small initial perturbations in the uni-

verse. In particular, the basic tool is the so called Press-Schechter formalism which considers the fraction of mass in the universe contained in gravitationally bound structures (such as galaxy clusters) with matter fluctuations greater than a critical value  $\delta_c$ . Assuming that the density contrast is normally distributed with zero mean and variance  $\sigma^2(\delta)$  we have:

$$dP(\delta) = \frac{1}{\sqrt{2\pi}\sigma} \exp\left[-\frac{\delta_c^2}{2\sigma^2(M, z)}\right] d\delta \quad (38)$$

where  $\delta_c$  is the linearly extrapolated density threshold above which structures collapse, ie,  $\delta_c = 1.686$ . Note, that it has been shown that  $\delta_c$  depends only weakly on  $\Omega_m$  (Eke, Cole & Frenk 1996). In this kind of studies it is common to parametrize the rms mass fluctuation amplitude at  $8 h^{-1}\text{Mpc}$  which can be expressed as a function of redshift as  $\sigma(M, z) = \sigma_8(z) = D(z)\sigma_8$ . The current cosmological models are normalized by the analysis of the WMAP 5 years data  $\sigma_8 = 0.80$  (Komatsu et al. 2009). The integration of eq.(38) provides the fraction of the universe, on some specific mass scale, that has already collapsed producing cosmic structures (galaxy clusters) at redshift  $z$  and is given by (see also Richstone et al. 1992):

$$P(z) = \frac{1}{2} \left[ 1 - \text{erf}\left(\frac{\delta_c}{\sqrt{2}\sigma_8(z)}\right) \right]. \quad (39)$$

Obviously the above generic of form eq.(39) depends on the choice of the background cosmology. The next step is to normalize the probability to give the number of clusters which have already collapsed by the epoch  $z$  (cumulative distribution), divided by the number of clusters which have collapsed at the present epoch ( $z = 0$ ),  $F(z) = P(z)/P(0)$ . In figure 5 we present in a logarithmic scale the behavior of normalized cluster formation rate as a function of redshift for the two cosmological models. In particular, for the traditional  $\Lambda$  cosmology we find the known behavior in which galaxy clusters appear to be formed at high redshifts  $z \sim 2$  (see for example Basilakos 2003 and references therein), while the same general picture seems to hold for the  $\Lambda(t)$  model. However, in the latter case we find the following differences: (i) clusters appear to form earlier ( $z \sim 3.5$ ) with respect to the  $\Lambda$  model and (ii) prior to  $z \sim 0.4$  the cluster formation has terminated due to the fact that the matter fluctuation field effectively freezes (see section 3.4). It is worth noting that the different formation rates between the two vacuum models, is due to the fact that the evolution of the corresponding growth factors are different (see the upper panel of figure 4). Finally, for a higher  $\sigma_8$  value ( $\sigma_8 = 0.95$ ) the corresponding cluster formation rate moves to higher redshifts [see figure 5:  $\Lambda(t)$ -open triangles and  $\Lambda$ -open points]. The opposite situation is true for  $\sigma_8 < 0.80$ .

## 6 CONCLUSIONS

In this paper we study analytically and numerically the large and small scale dynamical properties of the FLRW flat cosmologies in which the "vacuum" energy is a function of the cosmic time  $\Lambda(t)$ . Assuming that the



vacuum component can be expressed as a power series  $\Lambda = n_1 H + (3 - \beta)H^2$ , we find that the time evolution of the basic cosmological functions are described in terms of exponential functions which can accommodate a late time accelerated expansion, equivalent to the standard  $\Lambda$  model. Performing, a joint likelihood analysis using the current observational data (SNIa, CMB shift parameter and BAOs), we put tight constraints on the main cosmological parameters of the  $\Lambda(t)$  model. In particular, we find  $\Omega_m \simeq 0.29$ ,  $\beta \simeq 3.44$  and the age of the universe is  $t_0 \simeq 14.1 \text{Gyr}$  (for  $h = H_0/100 \simeq 0.705$ ). Also, we compare the  $\Lambda(t)$  scenario with the traditional  $\Lambda$  cosmology. We find that the behavior of the global expansion in the  $\Lambda(t)$  model compares well with that of the usual  $\Lambda$  cosmology. However, there are differences especially when we consider the small scale dynamics. Indeed, we reveal that the  $\Lambda(t)$  cosmological model has two important differences over the considered  $\Lambda$  cosmology:

- The amplitude and the shape of the linear growth of perturbations are different with respect to the  $\Lambda$  solution. As an example, prior to the inflection point the  $\Lambda(t)$  growth factor increases by a factor of  $\sim 43\%$ . In this context, the growth index of clustering ( $\gamma \simeq 0.50$ ) is somewhat different with that of the  $\Lambda$  model ( $\gamma_\Lambda \simeq 0.62$ ).
- The large scale structures (such as galaxy clusters) form earlier ( $z \sim 3.5$ ) with respect to those produced in the framework of the concordance  $\Lambda$  model ( $z \sim 2$ ).

## APPENDIX

In this appendix we treat analytically, as much as possible, the problem of the time varying  $\Lambda(t)$  parameter with the aid of a power series in  $H$  up to a third order:  $\Lambda = n_1 H + n_2 H^2 + n_3 H^3$  ( $n_3 \neq 0$ ). The time evolution equation for the Hubble flow is obtained by eq.(5) as:

$$\int_{+\infty}^H \frac{dy}{y(n_3 y^2 - \beta y + n_1)} = \frac{t}{2} \quad (40)$$

where  $\beta = 3 - n_2$ . In particular, the discriminant  $D = \beta^2 - 4n_1 n_3$  characterizes the solutions of eq.(40) as:

- *Case 1:*  $D > 0$  ( $\beta^2 - 4n_1 n_2 > 0$ ): The corresponding general solution of eq.(40) is written

$$\ln \left[ \frac{H^{\frac{1}{\rho_1 \rho_2}} (H - \rho_1)^{\frac{1}{\rho_1(\rho_1 - \rho_2)}}}{(H - \rho_2)^{\frac{1}{\rho_2(\rho_1 - \rho_2)}}} \right] = \frac{n_3 t}{2} \quad (41)$$

where  $\rho_{1,2} = \frac{\beta \pm \sqrt{D}}{2n_3} \neq 0$ . As an example for  $\beta = 0$  (or  $n_2 = 3$ ,  $\rho_1 = -\rho_2$ ) we obtain

$$H(t) = \frac{\rho_2}{\sqrt{1 - e^{n_3 \rho_2^2 t}}} \quad (42)$$

and

$$a(t) = a_1 \left( \frac{1 + \sqrt{1 - e^{n_3 \rho_2^2 t}}}{1 - \sqrt{1 - e^{n_3 \rho_2^2 t}}} \right)^{-\frac{1}{n_3 \rho_2}}, \quad (43)$$

where  $n_3 < 0$  and  $\rho_2 > 0$ . We would like to point out that as long as the cosmic time takes large values ( $t \gg$

1), the  $\Lambda(t)$  model has the de-Sitter feature due to  $a(t) \sim e^{\rho_2 t}$ . On the other hand, it is very interesting the fact that this model has no initial singularity. Indeed, for  $t \rightarrow 0$  we get  $a(t) \rightarrow a_1$ .

Now, if we consider  $\beta \neq 0$  then the situation becomes complicated (see eq.41) but for the special case of  $\rho_1 = 2\rho_2$  we can derive the following analytical solutions:

$$H(t) = \rho_2 + \frac{\rho_2}{\sqrt{1 - e^{n_3 \rho_2^2 t}}} \quad (44)$$

and

$$a(t) = a_1 e^{\rho_2 t} \left( \frac{1 + \sqrt{1 - e^{n_3 \rho_2^2 t}}}{1 - \sqrt{1 - e^{n_3 \rho_2^2 t}}} \right)^{-\frac{1}{n_3 \rho_2}} \quad (45)$$

where  $n_3 < 0$ ,  $\rho_2 > 0$  and  $\beta < 0$ . Again, the  $\Lambda(t)$  model asymptotically reaches the de-Sitter regime  $a(t) \sim e^{2\rho_2 t}$ , while for  $t \rightarrow 0$  we again find no singularity  $a(t) \rightarrow a_1$ .

- *Case 2:*  $D = 0$  ( $\beta^2 = 4n_1 n_3$ ): In this case the integration of eq.(40) leads to the solution of:

$$\ln \left( \frac{H}{H - \rho} \right) - \frac{\rho}{H - \rho} = \frac{\rho^2 n_3 t}{2} \quad (46)$$

where  $\rho = \frac{\beta}{2n_3} \neq 0$ . Now if  $\beta = 0$  ( $\rho = 0$ ), which implies that  $n_1 = 0$ , then the solution of eq.(40) is given by

$$H(t) = \sqrt{-\frac{1}{n_3 t}}, \quad n_3 < 0 \quad (47)$$

and

$$a(t) = a_1 e^{\sqrt{-\frac{4}{n_3} t}}. \quad (48)$$

- *Case 3:*  $D < 0$  ( $\beta^2 - 4n_1 n_2 < 0$ ): In this case the integration of eq.(40) leads to the solution of:

$$\ln \left( \frac{n_3 H^2}{n_3 H^2 - \beta H + n_1} \right) + \frac{2\beta}{\sqrt{-D}} \left[ \tan^{-1} G(H) - \frac{\pi}{2} \right] = n_1 t \quad (49)$$

where  $G(H) = (2n_3 H - \beta)/\sqrt{-D}$ .

## ACKNOWLEDGEMENTS

I thank the referee for his/her very detailed report, useful comments and suggestions.

## REFERENCES

- Alcaniz J. S., & Maia J. M. F., 2003, Phys. Rev. D., 67, 043502  
 Alcaniz J. S., & Lima J. A. S., 2005, Phys. Rev. D., 72, 063516  
 Arcuri R. C., & Waga, I., 1994, Phys. Rev. D., 50, 2928  
 Astier P., et al., 2006, A&A, 447, 31  
 Amendola L., Quercellini C., Tocchini-Valentini D., & Pasqui A., 2003, ApJ, 583, L53  
 Babić, A., Guberina, B., Horvat, R., & Stefancic, H., 2002, Phys. Rev. D., 65, 085002  
 Basilakos S., & Plionis M., 2005, MNRAS, 360, L35  
 Basilakos S., 2003, ApJ, 590, 636  
 Barrow J. D., & Clifton, T., 2006, Phys. Rev. D., 73, 103520  
 Bauer F., 2005, Class. Quant. Grav., 22, 3533  
 Bertolami O., 1986, Nuovo Cimento B, 93B, 36

- Bertolami O., & Martins P. J., 2000, Phys. Rev. D., 61, 064007
- Binder J.B., & Kremer G.M., 2006, Gen. Rel. Grav. 38, 857
- Bond, R. J., Efstathiou G. & Tegmark M., MNRAS, 1997, 291, L33
- Borges H. A., Carneiro, S., Fabris J. C., & Pigozzo, C., 2008, Phys. Rev. D., 77, 3513
- Bouso R., 2002, REv. Mod. Phys., 74, 825
- Cai R.G., & Wang A., 2005, JCAP, 0503, 002
- Caldwell R. R., Dave R., & Steinhardt P. J., 1998, Phys. Rev. Lett., 80, 1582
- Carneiro S., Dantas M. A., Pigozzo C., & Alcaniz J. S., 2008, Phys. Rev. D., 77, 3504
- Carvalho J. C., Lima J. A. S., & Waga I., 1992, Phys. Rev. D., 46, 2404
- Chevallier M., & Polarski D., 2001, Int.J. Mod. Phys. D., 10, 213
- da Angela J., et al., 2006, (astro-ph/0612401)
- Das, S., Corasaniti, P.S., & Khoury, J., 2006, Phys. Rev. D. 73, 083509
- Davis, T. M., et al., 2007, ApJ, 666, 716
- Efstathiou, G., 2002, MNRAS, 330, L29
- Eisenstein D. J., et al., 2005, ApJ., 633, 560
- Eke V., Cole S., & Frenk C. S., 1996, MNRAS, 282, 263
- Freedman, W., L., et al., 2001, ApJ, 553, 47
- Freese K., et al., 1987, Nucl. Phys., 287, 797
- Grande, J., Solá, J., & Stefancic, H., 2006, JCAP, 8, 11
- Hawkins E., et al., 2003, MNRAS, 346, 78
- Komatsu, E., et al., 2009, ApJS, 180, 330
- Kowalski, M., et al., 2008, ApJ, 686, 749
- Linder E. V., Phys. Rev. Lett., 2003, 90, 1301
- Martel H., & Wassermans I., 1990, ApJ, 348, 1
- McDonald, P., et al., 2005, ApJ, 635, 761
- Melchiorri, A., Mersini, L. Ödman, C. J., Trodden, M., 2003, Phys. Rev. D., 68, 043509
- Montenegro Jr., & Carneiro S., 2007 Class. Quant. Grav., 24, 313
- Mullis C. R., Rosati P., Lamer G., H. Böhringer, Schuecker P., & R. Fassbender R., 2005, MNRAS, 623, L85
- Nesseris, S., & Perivolaropoulos, L., 2007, JCAP, 0701, 018
- Nesseris, S., & Perivolaropoulos, L., 2008, Phys. Rev. D., 77, 3504
- Olivares, G., Atrio-Barandela, F., & Pavón, D., 2008, Phys. Rev. D., 77, 063513
- Opher R., & Pellison, A., 2004, Phys. Rev. D., 70, 063529
- Overduin J. M., & Cooperstock, F. I., 1998, Phys. Rev. D., 58, 043506
- Ozer M., & Taha, O., 1987, Nucl. Phys., B287, 776
- Padmanabhan, T., 2003, Phys. Rept., 380, 235
- Padmanabhan, T., 2005, Phys. Rept., 406, 49
- Padmanabhan N., et al., 2007, MNRAS, 378, 852
- Perlmutter, S., et al., 1999, ApJ, 517, 565
- Peebles P.J.E., 1984, ApJ, 284, 439
- Peebles P. J. E., & Ratra, B., 1988, ApJ, 325, L17
- Peebles, P. J., E., 1993, Principles of Physical Cosmology, Princeton University Press, Princeton New Jersey
- Peebles, P. J. E., & Ratra, B., Rev.Mod.Phys., 2003, 75, 559
- Ratra, B., & Peebles P. J. E., 1988, Phys. Rev. D, 37, 3406
- Ray, S., Mukhopadhyay, U, & Meng, Xin-He, Grav. Cosmol., 2007, 13, 142
- Richstone D., Loeb A., & Turner E. L., 1992, ApJ, 393, 477
- Riess, A. G., et al., 1998, AJ, 116, 1009
- Ross N. P., et al., 2006, (astro-ph/0612400)
- Shapiro, I. L., & Solá, J., 2000, Phys. Lett. B., 475, 236
- Sil, A., & Som, S., Astrophys. & Space Science, 2008, 318, 109
- Stanford S. A., et al., 2006, ApJ, 646, L13
- Tegmark, M., et al., 2006, Phys. Rev. D., 74, 123507
- Trotta, R., 2004, Cosmic Microwave Background Anisotropies: Beyond Standard Parameters, (astro-ph/0410115)
- Turner M. S., & White M., 1997, Phys. Rev. D, 56, R4439
- Verde L., et al., 2002, MNRAS, 335, 432
- Wang L., & Steinhardt P.J., 1998, ApJ, 508, 483
- Wang P., & Meng, X., 2005, Clas. Quant. Grav., 22, 283
- Weinberg S., 1987, Phys. Rev. Lett., 59, 2607
- Weinberg S., 1989, Rev. Mod. Phys., 61, 1
- Zimdahl W., Pavón D., Chimento, L.P., 2001, Phys.Lett.B, 521, 133